Arginine Activity in the Proton-Motive Photocycle of Bacteriorhodopsin: Solid-State NMR Studies of the Wild-Type and D85N Proteins†

Aneta T. Petkova,‡,§ Jingui G. Hu,‡,§ Marina Bizounok,‡ Michelle Simpson,‡ Robert G. Griffin,§ and Judith Herzfeld*,‡

Department of Chemistry and Keck Institute for Cellular Visualization, MS #015, Brandeis University, Waltham, Massachusetts 02454-9110, and Department of Chemistry and Francis Bitter Magnet Laboratory, Massachusetts Institute of Technology, Cambridge, Massachusetts 02139

Received August 17, 1998; Revised Manuscript Received November 23, 1998

ABSTRACT: ^{15}N solid-state NMR (SSNMR) spectra of guanidyl-^{15}N-labeled bacteriorhodopsin (bR) show perturbation of an arginine residue upon deprotonation of the retinal Schiff base during the photocycle. At the ϵ position, an upfield shift of 4 ppm is observed while the η nitrogens develop a pair of 'wing' peaks separated by 24 ppm. Proton-driven spin diffusion between the two 'wing' peaks indicates that they arise from a single Arg residue. An unusually asymmetric environment for this residue is indicated by comparison with guanidyl-^{15}N chemical shifts in a series of arginine model compounds. The 'wing' peaks are tentatively assigned to Arg-82 on the basis of the SSNMR investigations of the alkaline and neutral dark-adapted forms of the D85N bacteriorhodopsin mutant. Another, less asymmetric pair of η signals, that is not affected by Schiff base deprotonation or D85 mutation, is tentatively assigned to Arg-134. The results are discussed in relation to existing models of bR structure and function.

Arginine is one of the most hydrophilic amino acids in proteins, and hence Arg residues are often found at or near the surfaces of proteins. Arginine is also the most basic amino acid (pK_a ∼13), with delocalization of the positive charge greatly facilitated by the planar "y" shape of the protonated guanidinium group ["y-aromaticity" (*1*)]. Arginine residues which are buried in the interior of proteins are likely to be involved in the formation of stabilizing salt bridges or strong H-bonds between helices (*2*). The five nitrogen-bonded protons of the guanidinium group are capable of participating in four types of geometrically specific interactions with carboxylate or phosphate groups (*3*), thus permitting molecular recognition. For example, arginine has often been found at the recognition sites for phosphate-containing substrates and cofactors (*4, 5*), and has been proposed to participate in phosphoryl transfer reactions (*6, 7*). Arginine residues in nucleic acid binding proteins reportedly can form nonspecific ion pairs with the phosphate backbone as well as sequence-specific H-bonds with the bases (*8, 9*).

Bacteriorhodopsin (bR)[1] is a trans-membrane protein found in the purple patches of the plasma membrane of *Halobacterium salinarium* (formerly also known as *Halobacterium halobium*). The 26 kDa protein contains 248 amino acid residues, forming a 7-helix bundle, and a retinal chromophore situated in the middle, covalently bound to Lys-216 via a Schiff base (SB) linkage. The bR structure deduced from electron cryomicroscopy studies of the two-dimensional crystals in the native purple membrane (*10*−*12*), and from X-ray studies of microcrystals grown in lipidic cubic phases (*13, 14*), shows that in the resting state of the protein most of the ionizable residues (Asp, Glu, Arg, and Lys) are very close to or at the membrane surface. The exceptions are Asp-96, Asp-115, Asp-212, Asp-85, and Arg-82. The first two of these residues are protonated in the resting state of the protein (*15*), while the last three residues, together with one or more water molecules, form the complex counterion of the protonated Schiff base (*16*−*19*).

Bacteriorhodopsin functions as a light-driven proton pump (*20*−*22*). Photoisomerization of the all-trans bR_{568} chromophore to a 13-cis conformation is followed by deprotonation of the Schiff base and protonation of Asp-85, release of a proton at the extracellular surface, reprotonation of the SB from Asp-96, proton uptake from the cytoplasmic side, reprotonation of Asp-96, reisomerization of the chromophore, and deprotonation of Asp-85 to complete the photocycle. The exact sequence of some these processes depends on the experimental conditions, i.e., pH, salt, temperature, etc. Net proton transfer from the cytoplasmic side to the extracellular side of the membrane creates an electrochemical potential gradient which is used by the *Halobacterium salinarium* cell for metabolic purposes.

The bR structure (*11*−*14*) places the seven arginine residues as follows: Arg-7 in the N-terminus, just before the onset of helix A on the extracellular side of the

† This research was supported by the National Institutes of Health (GM-36810, GM-23289, and RR-00995).

* To whom correspondence should be addressed. E-mail: herzfeld@brandeis.edu.

‡ Brandeis University.

§ Massachusetts Institute of Technology.

[1] Abbreviations: bR, bacteriorhodopsin; CP, cross-polarization; DA, dark-adapted resting state of bR; Gdn·HCl, guanidine hydrochloride; LA, light-adapted resting state of bR in which the Schiff base (SB) is protonated and Asp-85 is deprotonated; M_o and M_n, succeeding bR photocycle intermediates in which the SB is deprotonated; N and O, succeeding photocycle intermediates in which the SB is reprotonated; MAS, magic angle spinning; NMR, nuclear magnetic resonance; SB, Schiff base; SSNMR, solid-state NMR; WT, wild type.

10.1021/bi981968z CCC: $18.00
Published on Web 01/14/1999

membrane; Arg-82 in helix C; Arg-134 at the very beginning of helix E on the extracellular side of the membrane; Arg-164 in the E−F loop; Arg-175 in the cytoplasmic half of helix F; and Arg-225 and Arg-227 on the cytoplasmic side of the membrane, at the end of helix G and beginning of the C-terminus, respectively. Site-specific mutations of all seven arginines have been studied extensively in order to explore the roles that these residues might play in the photocycle. The three mutants obtained after substitution of arginine with glutamine at positions 7, 164, and 225 (R7Q, R164Q, and R225Q) showed essentially the wild-type phenotype in regard to chromophore regeneration, λ_{max}, and proton pumping, indicating no involvement in the WT photocycle as might be expected for residues at or near the protein surface (*23, 24*). However, in the R175Q mutant, the rate of chromophore regeneration was substantially decreased, and the rate of reprotonation of the SB was greatly increased, suggesting that Arg-175 might be involved in the folding pathway of bR (*24*). The R227Q mutant showed reduced proton pumping ability and unusually slow decay of the M photointermediate, resulting from a decreased entropy of activation (combined with a decreased energy of activation similar to that observed in mutants of Asp-96, the internal proton donor). It was suggested (*24*) that removing the positive charge of Arg-227 could disturb the proton-conducting network in the cytoplasmic half of the channel, resulting in inhibition of reprotonation of the SB. Both the R134Q and R134C mutants showed somewhat reduced extents of chromophore regeneration and light adaptation. The photocycle kinetics were similar to WT (*23, 24*) for Arg-134 mutations expressed in *Halobacterium salinarium* as well as in *E. coli*. However, the proton pumping efficiency was substantially reduced, and, in *H. salinarium*, the ratio of unfolded bR in the cytoplasm to folded bR in the membrane was significantly increased in R134K, R134A, and R134Q, indicating the importance of Arg-134 in stabilizing the structure of bR (*25*). A more recent study of R134K (*26*) found a smaller pK_a difference between D85 and the proton release group, which suggests a weaker coupling between these two groups. In the electron microscopy based model of Grigorieff et al. (*11*), a salt bridge has been built between Arg-134 and Glu-194.

As already mentioned, Arg-82 is a part of the complex counterion of the retinal SB. Replacement of Arg-82 by uncharged residues, in both *E. coli* and *H. salinarium*, produces a red shift in the chromophore absorption at neutral pH and substantial delays in proton release (*23, 27, 28*). The characteristics of these species are similar to the WT blue membrane, obtained by deionization or acidification, and suggest an increase in the pK_a of Asp-85. This change in the pK_a could be explained by an electrostatic interaction between the side chains of Arg-82 and Asp-85 which would be abolished in the absence of the positive charge at position 82 in the mutants. Photocurrent and pH indicator dye measurements of the photocycle of Arg-82 mutants suggest that R82 regulates the pK_a of the proton release group in the unphotolyzed state and the M photointermediate (*29, 30*). Furthermore, the pH dependence of the rate of dark-adaptation (all-trans,15-anti→13-cis,15-syn thermal isomerization) reflects the pK_a's of Asp-85 and the extracellular proton release group, and suggests a coupling between these two groups which is modulated by the nature of the residue at position 82 (*27, 28, 30, 31*). It has been proposed that this linkage might be a part of the "reprotonation switch" of bR (*32, 33*), and might be controlled by a flip of the flexible Arg-82 side chain. Such a flip has been suggested by molecular dynamics simulations for the bR photocycle (*34−36*): in the resting state of the protein, the side chain of Arg-82 is oriented toward Asp-85, and upon protonation of Asp-85, it is moved gradually (through a series of M intermediates) toward the extracellular surface to complete the change upon the deprotonation of Glu-204. In the photoactive yellow protein, a conformational change of an arginine side chain has been observed by millisecond time-resolved crystallographic studies (*37*): as an example of gating, the side chain of Arg-52 moves away from the phenolic chromophore, in the transition between the dark state and the photostationary state, thus allowing solvent access and protonation of the chromophore.

The D85N mutant of bR is of special interest as a model for the WT photocycle intermediates M, N, and O in which Asp-85 is protonated. In fact, a pH-dependent equilibrium between three species is observed in dark-adapted D85N bR (*38−40*). In 0.1 M NaCl, a yellow M-like form with a deprotonated SB predominates at alkaline pH, while a blue O-like form with a protonated SB prevails in acidic media. Illumination of the M-like species with blue light induces a photocycle with proton transport in the same direction as in the wild-type (*39, 41*).

While a good deal is known about the proton-motive photocycle of bR, the detailed molecular mechanism of proton gating remains to be elucidated. Solid-state NMR spectroscopy can make an important contribution through its ability to probe the state and interactions of isotopically labeled sites and measure internuclear distances among sites. In the present solid-state NMR study, we follow changes in the guanidyl groups of the seven arginine residues in bR in the transition from the light-adapted (LA) state to the early and late M photointermediates, M_o and M_n. We identify a residue which shows extremely asymmetric interactions in the two wild-type M states. Similar interactions for this residue are observed in the alkaline and neutral forms of the D85N mutant of bR. Current models of the bR structure and photocycle favor the assignment of this residue to Arg-82. A second asymmetric arginine residue which does not change in the observed photocycle states is tentatively assigned to Arg-134.

MATERIALS AND METHODS

Figure 1 shows the current nomenclature used in labeling the atoms of arginine.

Model Compounds. Model compounds were identified for which crystal structures exist (Cambridge Structural Database). L-Arg (free base), L-Arg·HCl, L-Arg-L-Asp, L-Arg-L-Glu, L-ascorbic acid, and *N*-benzyloxycarbonyl-L-Arg (abbreviated as N-BzC-Arg) from Sigma Chemical Co. (St. Louis, MO) and L-[U-^{13}C,^{15}N]Arg·HCl, L-[$\eta_{1,2}$-$^{15}N_2$]Arg·HCl, and [1,1′-$^{13}C_2$]acetic anhydride from Cambridge Isotope Laboratories (Andover, MA) were used in the preparation of the model compounds. The crystals of Arg·2H_2O, Arg·HCl, Arg·HCl·H_2O, Arg·HBr·H_2O, Arg·H_3PO_4·H_2O, N-BzC-Arg·$^1/_2H_2O$, Arg-Asp·H_2O, Arg-Glu·H_2O, and Arg ascorbate were each prepared as reported for their respective crystal structure studies (*42−49*). *N*-Acetyl-L-arginine (N-Ac-Arg)

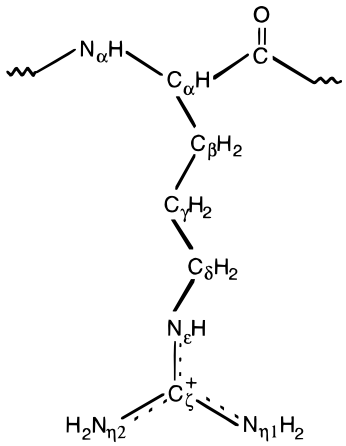

FIGURE 1: Structure and nomenclature for arginine. With a pK_a ~13, the guanidyl group is protonated and planar under most conditions.

was synthesized via a slight modification of the method suggested in (*50*). Crystals of N-Ac-Arg·2H_2O were obtained by slow cooling of an aqueous solution of N-Ac-Arg from ~60 °C to room temperature. A frozen sample of saturated aqueous [$\eta_{1,2}$-$^{15}N_2$]Arg·HCl titrated at room temperature to pH 13.8 with concentrated KOH was also used.

Bacteriorhodopsin. Wild-type bR was biosynthetically labeled with L-[$\eta_{1,2}$-$^{15}N_2$]Arg by using an arginine auxotrophic strain of *Halobacterium salinarium*, grown in a synthetic medium similar to (*51*). The arginine auxotroph was prepared by repeated antibiotic enrichment with bacitracin, followed by replica plating, using otherwise standard procedures (*52*, *53*). The co-incorporation of [ζ-^{14}C]Arg as a radioactive tracer enabled us to conclude from extraction and amino acid analysis that 90% labeling of the guanidyl group was achieved with no scrambling to other amino acid residues, lipid or chromophore.

[ϵ-^{15}N]Arg-bR was produced by replacing arginine in the culture medium of the R-1 strain with L-[ϵ-^{15}N]ornithine. Trace L-[2,3-$^3H_2$]ornithine was also introduced in the medium in order to estimate the incorporation rate of the ϵ-^{15}N-labeled ornithine. The arginine residues were approximately 75% labeled with no scrambling to other amino acid residues, lipid or chromophore.

[ζ-^{15}N]Lys-bR was prepared by replacement of natural-abundance L-Lys in the growth medium with 0.085 g/L L-[ζ-^{15}N]Lys. Co-incorporation of L-[4,5-$^3H_2$]Lys in the medium enabled us to determine that the lysines were ~70% labeled with no scrambling to other amino acid residues. However, ~40% of the incorporated radioactive label was found with the lipids and the chromophore upon extraction.

[1-^{13}C]Ala,[U-^{13}C,^{15}N]Arg,[ζ-^{15}N]Lys-bR and [1-^{13}C]Ala,-[U-^{15}N]Arg,[ζ-^{15}N]Lys-bR were prepared by growing the arginine auxotrophic strain of *Halobacterium salinarium* in the usual medium to which L-[1-^{13}C]Ala, L-[U-^{13}C,^{15}N]Arg, or L-[U-^{15}N]Arg, and L-[ζ-^{15}N]Lys were supplied instead of the unlabeled amino acids. The incorporation of the labeled amino acids was traced with L-[1-^{14}C]Ala, L-[ζ-^{14}C]Arg, and L-[4,5-$^3H_2$]Lys, and was shown to be ~80%, ~90%, and ~55%, respectively. No scrambling of the radioactive label to other residues in the protein were detected, although ~45% of the radioactivity incorporated from L-[1-^{14}C]Ala and ~50% of the radioactivity incorporated from L-[4,5-$^3H_2$]Lys was found with the lipids and the chromophore upon extraction.

The D85N mutant (strain kindly provided by Prof. R. Needleman, Wayne State University, Detroit, MI) was generally ^{15}N-labeled from 94% $^{15}NH_4Cl$ in the growing medium. This method yields sufficient labeling of the η nitrogens of the arginine residues for detection of the resonances without interference from the strong amide signal (see below).

The purple (WT) and blue (D85N) membranes were isolated and purified in the usual manner (*54*). However, the sucrose gradient of the lysed D85N membranes showed two blue bands. Only the protein from the band that had migrated to the denser position was used in the experiments. The sucrose was removed by washing several times with deionized H_2O. The sample was then washed 3−4 times with the final medium. After the last centrifuge spin (90 min at 30000*g*), the bR pellet was packed in a transparent 7-mm sapphire rotor with transparent Kel-F endcaps (Doty Scientific, Columbia, SC), or in a 5-mm zirconia rotor (Chemagnetics, Ft. Collins, CO).

Light was delivered to the sample via a glass optic fiber bundle (*55*), with the end positioned at the top stator endcap of the 7-mm spinner module, or at the middle of the 5-mm spinner module. LA was obtained after 3−4 h of illumination of WT, at 1 to −2 °C, with white light from a 1000 W Xe lamp (Oriel Instruments, Stratford, CT), directed through a water filter and an IR blocking filter (Oriel Instruments) to reduce heating. The M_o and N photointermediates were accumulated by illumination of LA in 0.1 M NaCl, pH 10.0−10.2, with $\lambda > 550$ nm (long-pass filter from Oriel Instruments) for 1 h at temperatures between −15 and −80 °C. Alternatively, in 0.3 M Gdn·HCl, pH 10, 1 h irradiation of LA with $\lambda > 550$ nm at temperatures between −20° and −60 °C yielded varying mixtures of N, M_n, M_o, and residual LA. Once accumulated, photocycle intermediates were preserved in the dark between −80 and −130 °C for the duration of data acquisition. The alkaline and neutral forms of D85N were observed in their dark-adapted state.

Solid-State NMR. Spectra of WT and D85N bR were acquired at spinning frequencies between 3 and 5 kHz, using a custom-built spectrometer operating at 7.4 T (^{15}N, ^{13}C, and ^{1}H frequencies of 32.2, 79.9, and 317.6 MHz, respectively). Two different variable-temperature probes were used for the experiments: a double resonance probe equipped with a 7-mm Doty MAS spinner module, and a quadruple resonance transmission line probe equipped with a 5-mm Chemagnetics spinner module and a stainless-steel dewar for lower temperatures. The temperature calibration was performed by monitoring the ^{207}Pb resonance of $Pb(NO_3)_2$ (*56*). The spectra were obtained by standard cross-polarization (CP) (*57*) under MAS, with CW or TPPM (*58*) decoupling, with or without a $\pi/2$ flip back pulse (to compensate for the long T_1's of the arginine model compounds). Delayed CP ($90°-\tau_d/2-180°-\tau_d/2-\tau_{CP}$−decouple on the ^{1}H channel) (*59*) was used to probe for bR protons in rapid exchange with bulk water. The peak inversion in the spin diffusion experiments was achieved by the rotor-synchronized DANTE sequence (*60*). The carrier was centered at the resonance to be inverted, and a train of four $\pi/4$ (model compound) or eight $\pi/8$ (bR) pulses was applied on the ^{15}N channel, followed by a mixing time during which the ^{1}H decoupling power was removed.

Table 1: ^{15}N Isotropic Chemical Shifts of Arginine-Containing Compounds

compound	δ_α	δ_ϵ[b]	$\delta_{\eta 1}$[b]	$\delta_{\eta 2}$[b]	$\delta_{\eta 1} - \delta_{\eta 2}$[c]
N-Ac-Arg·2H$_2$O	111.2	60.0	51.5	34.2	17.3
Arg·2H$_2$O	9.7	61.0	51.5	44.3	7.2
Arg·HCl[a]	16.9	63.9, 62.8	57.9, 54.8	41.2, 39.6	16.7, 15.2 or 18.3, 13.6
Arg·HCl·H$_2$O[a]	18.0	63.6	55.2	41.2, 40.0	15.2, 14.0
Arg·HBr·H$_2$O[a]	19.9, 17.3	67.4	62.0, 59.0	43.1	18.9, 15.9
Arg·H$_3$PO$_4$·H$_2$O	12.1	57.3	47.8	42.9	4.9
N-BzC-Arg·$^1/_2$H$_2$O[a]	*d*	68.9, 63.5	52.2, 50.3	46.8, 43.4	5.4, 6.9 or 8.8, 3.5
Arg-Asp·H$_2$O	*d*	56.3	51.4	42.3	9.1
Arg-Glu·H$_2$O	*d*	57.5	48.8	42.7	6.1
Arg ascorbate	11.9	57.8	45.6	44.5	1.1
Arg, pH 13.8, −80 °C	*e*	*e*	51.6	43.3	8.3
range	−	68.9−56.3	62.0−45.6	46.8−34.2	18.9−1.1

[a] The crystal structure indicates the presence of two molecules in the unit cell, which give rise to distinct NMR signals for some of the positions in the molecule. [b] The guanidinium group resonances are assigned as ϵ, η_1, and η_2 according to decreasing chemical shifts. [c] In the two cases where four resonances were detected for the terminal nitrogens, the two possibilities for the $\delta_{\eta 1} - \delta_{\eta 2}$ differences are given. [d] Absence of resonance may be due to interference between proton exchange and decoupling (*81*). [e] Resonance is not observed due to the lack of label.

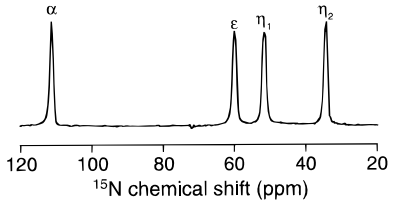

FIGURE 2: ^{15}N CP/MAS spectrum of *N*-[1-^{13}C]acetyl-[U-^{13}C,^{15}N]-Arg·2H$_2$O (~13% isotopic enrichment).

Typical $\pi/2$ pulse lengths were 2.5−3.5 μs for ^{1}H and 5.5−6.5 μs for ^{15}N. The usual TPPM pulse angle and phase were 170° and 45°, respectively. Spectra were collected with 2 ms CP contact time, 1024 acquisition data points, and 20 μs dwell time. The recycle delay was 3 s for bR and 10−15 s for the arginine model compounds. A total of 20 000 to 36 000 scans were averaged for each ^{15}N spectrum of WT and D85N bR (unless otherwise noted). ^{13}C and ^{15}N chemical shifts are externally referenced to TMS and 5.6 M aqueous ^{15}NH$_4$Cl, respectively, and bear a 0.4 ppm uncertainty.

RESULTS

In preparation for studying the Arg-labeled bR samples, we examined spectra of a large number of model compounds. A compilation of the measured ^{15}N chemical shifts is presented in Table 1, and a typical ^{15}N CP/MAS spectrum, that of *N*-[1-^{13}C]acetyl-[U-^{13}C,^{15}N]Arg·2H$_2$O, is shown in Figure 2. With an amide linkage and hydration, N-Ac-Arg·2H$_2$O is a good model system for many peptides and proteins. The X-ray and neutron diffraction derived crystal structures of the model compounds show zwitterions with a positively charged, planar guanidinium group, a deprotonated carboxyl group (where present), and a protonated amino group if a second negative charge is available in the crystal. All the nitrogen atoms were found to participate in H-bonds. The chemical shifts of the ϵ nitrogens range from 68.9 to 56.3 ppm, while the η chemical shifts range from 62.0 to 45.6 ppm for the downfield resonance and from 46.8 to 34.2 ppm for the upfield resonance.

A summary of the ^{13}C measurements is presented in Table 2, and the ^{13}C CP/MAS spectrum of *N*-[1-^{13}C]acetyl-[U-^{13}C,^{15}N]Arg·2H$_2$O is shown in Figure 3. The chemical shifts of the carbon atoms vary as follows: COO$^-$/CO, 182.9−167.2; C$_\zeta$, 159.4−156.0; C$_\alpha$, 59.6−53.6; C$_\delta$, 45.4−39.3; C$_\beta$, 32.5−27.5; and C$_\gamma$, 28.3−21.4 ppm. The ζ carbon shows a very small chemical shift range and a single resonance, even in the cases where two different crystal forms coexist with different ϵ-^{15}N and η-^{15}N chemical shifts.

The ^{15}N CP/MAS spectrum of [$\eta_{1,2}$-^{15}N$_2$]Arg-bR in the LA state (Figure 4, top) shows a relatively broad (fwhm = 7.7 ppm) resonance, centered at 45.9 ppm. Except for a downfield shoulder at 55.6 ppm, there is no apparent resolution of the 14 η signals (from the 7 arginine residues) in bR. This situation changes dramatically in the spectrum of the M$_o$ photointermediate cryo-trapped at −44 °C (Figure 4, middle). Two resonances emerge, at 60.1 and 36.4 ppm. We refer to these new features as 'wing' peaks, or simply 'wings' to reflect their position with respect to the broad (fwhm = 8.7 ppm) arginine resonance at 45.9 ppm. The LA − M$_o$ difference spectrum (Figure 4, bottom) shows that the nitrogens with 60.1 and 36.4 ppm shifts in M$_o$ have shifts of 48.1 and 45.9 ppm in LA.

[ζ-^{15}N]Lys-bR has been used to identify the bR photointermediates cryo-trapped at different temperatures, since the SB nitrogen exhibits distinctive ^{15}N chemical shifts for the DA, LA, L, M$_o$, M$_n$, and N states (*18, 55, 61*−*63*). ^{15}N CP/MAS spectra of [$\eta_{1,2}$-^{15}N$_2$]Arg-bR and [ζ-^{15}N]Lys-bR were obtained under identical conditions (0.1 M NaCl, pH 10.1), and the relative peak intensities extracted from the data were plotted in Figure 5. It should be noted that the error in the fraction of each intermediate is difficult to assess owing to differences in the CP matching conditions for the various species. Nevertheless, an obvious conclusion from the plot is that the 'wing' peaks track with the M$_o$ photointermediate. ^{15}N CP/MAS investigations of [$\eta_{1,2}$-^{15}N$_2$]Arg-bR in 0.3 M Gdn·HCl at pH 10 established the presence of the same 'wing' peaks in the M$_n$ intermediate as well (results not shown).

Accounting for the populations of the two states in Figure 4, one can estimate from the difference spectrum that the relative intensity of the 'wing' peaks corresponds to 2 of the 14 η nitrogens in the 7 Arg residues of bR. Proton-driven spin diffusion was employed in order to investigate whether the two 'wings' arise from the same arginine residue. The procedure was tested in [$\eta_{1,2}$-^{15}N$_2$]Arg·HCl·H$_2$O (>95%), where the chemical shift separation between the η nitrogens is 15 ppm. The rotor-synchronized DANTE sequence was used to invert the downfield peak, and the decay of the

Table 2: ^{13}C Isotropic Chemical Shifts of Arginine-Containing Compounds

compound	δ_{CO}	δ_ζ	δ_α	δ_δ	δ_β	δ_γ
N-Ac-Arg·2H$_2$O[a]	178.4, 177.8	156.2, 156.0	58.5, 58.3	41.5, 41.3	28.2	25.9
Arg·2H$_2$O	182.9	159.4	56.7	43.6	32.5	25.1
Arg·HCl[a,b]	177.0, 176.3, 175.8, 175.1	157.3	57.0, 55.0	42.5, 41.5	29.8, 28.3	25.8, 22.8
Arg·HCl·H$_2$O[b]	176.8, 174.8	156.3	54.9	41.5	27.5	24.4
Arg·HBr·H$_2$O[b]	177.7, 176.0	159.4	59.6, 57.0	45.4, 44.4	30.1, 29.7	27.5, 24.7
Arg·H$_3$PO$_4$·H$_2$O	177.5	156.4	56.7	39.4	28.3	28.3
N-BzC-Arg·$^1/_2$H$_2$O[b]	181.5	156.8	56.5	42.5, 41.2	32.2, 28.4	25.8, 23.6
Arg-Asp·H$_2$O	168.0	157.2	53.6	39.3	30.0	22.2
Arg-Glu·H$_2$O[c]	167.2	157.6	56.2	44.0	33.5, 30.6 or 28.9	21.4
Arg ascorbate	175.7	158.1	54.7	41.5	28.9	22.9
range	182.9−167.2	159.4−156.0	59.6−53.6	45.4−39.3	32.5−27.5	28.3−21.4

[a] The splittings arise from the *J* couplings in these uniformly labeled samples. [b] Two molecules per unit cell produce multiple resonances. [c] Three possible chemical shifts are listed for C_β, because δ_β and δ_γ of Glu are in the same region, as has been observed by others.

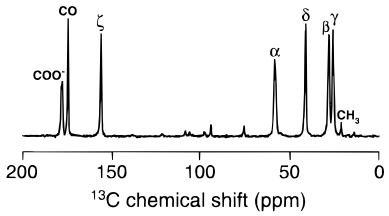

FIGURE 3: ^{13}C CP/MAS spectrum of *N*-[1-^{13}C]acetyl-[U-^{13}C,^{15}N]-Arg·2H$_2$O (∼13% isotopic enrichment). The COO$^-$, C_ζ, C_α, and C_δ resonances show *J* coupling-induced splittings.

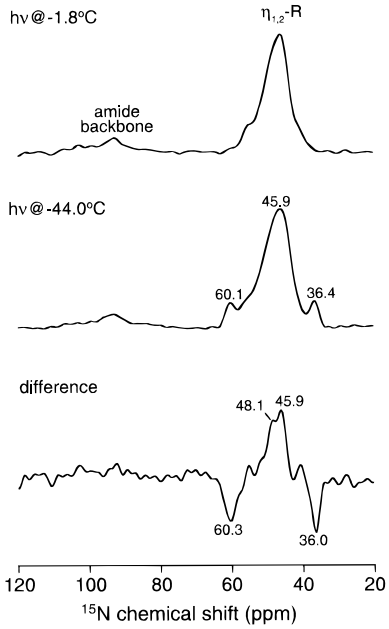

FIGURE 4: ^{15}N CP/MAS spectra of [$\eta_{1,2}$-^{15}N$_2$]Arg-bR in 0.1 M NaCl at pH 10.1 after irradiation at −1.8 °C with white light to light-adapt (top), and then further at −44.0 °C with λ > 550 nm to accumulate M_o (middle). No resolution of the seven arginine residues in bR is observed in the resting state (LA), but two 'wing' peaks at 60.1 and 36.4 ppm appear in the M_o photocycle intermediate. The difference spectrum expanded 4.5 times (bottom) shows that the perturbed nitrogens have chemical shifts of 48.1 and 45.9 ppm in LA.

magnetization with respect to the mixing time in the DANTE−0° and DANTE−180° case is plotted in Figure 6. There is virtually no decay in the control case, which indicates a long ^{15}N T_1. In contrast, after 1 s of spin diffusion approximately 65% decay is observed. The rate of spin diffusion reflects the distance between the two coupled spins, which is 2.3 Å in [$\eta_{1,2}$-^{15}N$_2$]Arg·HCl·H$_2$O.

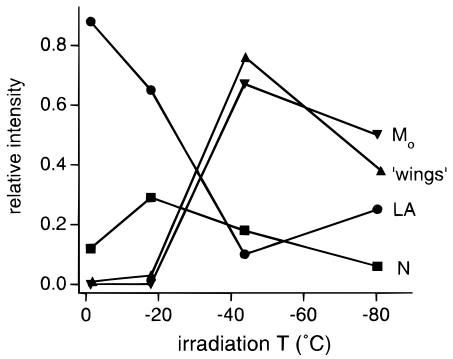

FIGURE 5: Relative intensities of the arginine [$\eta_{1,2}$-^{15}N] 'wing' peaks and the LA, M_o, and N [ζ-^{15}N]Lys Schiff base signals in spectra obtained as in Figure 4 but with irradiation of LA at different temperatures. The 'wing' peaks track with the M_o state.

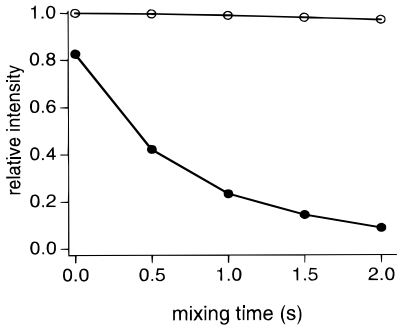

FIGURE 6: Test of spin diffusion in [$\eta_{1,2}$-^{15}N$_2$]Arg·HCl·H$_2$O. The filled circles (●) represent data for inversion and spin diffusion, while the open circles (○) correspond to mixing without inversion. The sum of the absolute intensities of the two peaks is normalized to the first point in the control experiment.

The results of the same experiment on the 'wing' peaks of bR are presented in Figure 7. We were able to invert the downfield 'wing' peak [the accurate frequency was determined from the M_o − LA CP difference spectrum (as in Figure 4)], leaving the broad arginine resonance, the upfield 'wing', and the backbone peak unaffected (Figure 7, middle). After 1.1 s mixing achieved via spin diffusion, the intensity of the 'wing' peaks was substantially decreased (Figure 7, bottom). To clarify the change induced by spin diffusion, the difference spectrum between the 0 and 1.1 s mixing times, (i.e., the amount of magnetization that dephased owing to spin diffusion) is shown in Figure 8, top spectrum. The corresponding spectrum obtained from the same experiments in the LA state is shown in Figure 8, middle spectrum. It is apparent that the CPDANTE pulse train had inverted the

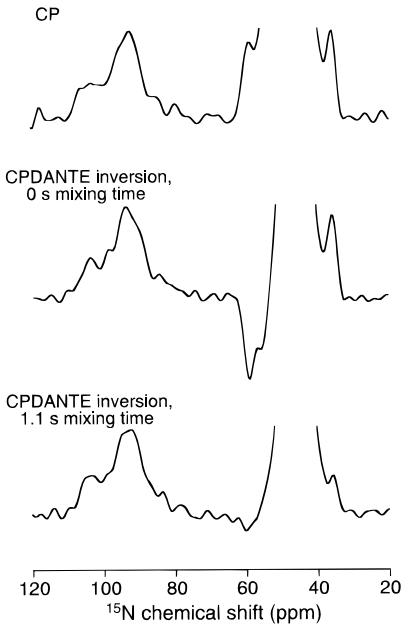

FIGURE 7: Spin diffusion between the 'wing' peaks of [$\eta_{1,2}$-^{15}N]-Arg-bR in the M_o state, accumulated in 0.1 M NaCl at pH 10 by illumination of LA with $\lambda > 550$ nm at −65 °C: standard CP spectrum (top); DANTE inversion of the downfield 'wing' peak without mixing (middle spectrum); and spin diffusion after 1.1 s mixing (bottom spectrum). The intensity of the 'wings' is diminished to an extent similar to the model compound at 1.0 s mixing time (see Figure 6), indicating that the nitrogens giving rise to the 'wing' peaks belong to a single arginine residue in bR.

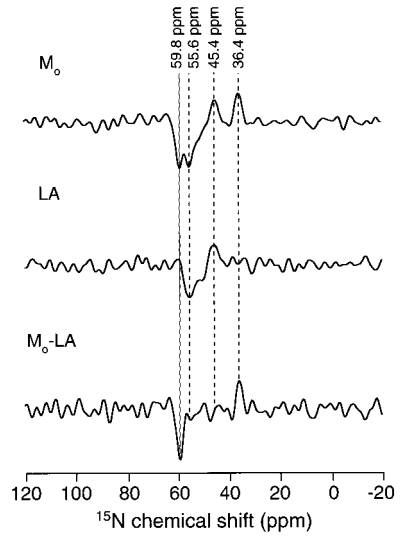

FIGURE 8: ^{15}N difference (mixing minus no mixing) spectra illustrating the reduction of peak intensity during the 1.1 s spin diffusion period in [$\eta_{1,2}$-^{15}N]Arg-bR in 0.1 M NaCl, pH 10: the M_o photointermediate (top); the LA photointermediate (middle); and M_o − LA (bottom). Even though the downfield peaks of two pairs of η nitrogens have been inverted in the M_o state, the pair involving the 55.6 ppm peak is not changed in the LA to M_o transition.

downfield 'wing' peak together with the downfield shoulder. However, the difference between the M_o and LA spectra (Figure 8, bottom) clearly indicates that the spin pair including the downfield shoulder does not change in this photocycle transition, and that spin diffusion of 1.1 s produces approximately 60% reduction of the intensity of the 'wing' peaks. This is consistent with the $\eta_1 - \eta_2$ internuclear distance within a guanidyl group based on the

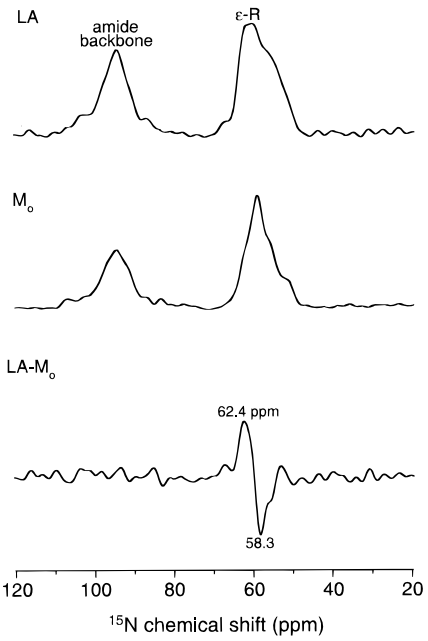

FIGURE 9: ^{15}N CP/MAS spectra of [ϵ-^{15}N]Arg-bR in 0.1 M NaCl at pH 10: LA state (top spectrum); M_o state (middle spectrum); and the difference spectrum between M_o and LA (bottom). An upfield shift of about 4 ppm is detected in the LA to M_o transition, with an intensity consistent with perturbation of one of the seven arginines.

model study. Therefore, the two 'wings' arise from nitrogen atoms of the same arginine residue in bR. At the same time, the unperturbed arginine residue responsible for the 55.6 ppm shoulder in Figure 4 is shown to also be responsible for a N_η signal at 45.4 ppm.

Perturbation of an arginine residue in the LA→M_o transition is also apparent in spectra of the ϵ nitrogens. ^{15}N CP/MAS spectra of LA and M_o states of the [ϵ-^{15}N]Arg-bR photocycle in 0.1 M NaCl and pH 10 are shown in Figure 9, top and middle. The difference spectrum (Figure 9, bottom) shows an upfield shift of 4 ppm in the LA→M_o transition.

The ^{13}C resonances of [1-^{13}C]Ala,[U-^{13}C,^{15}N]Arg,[ζ-^{15}N]-Lys-bR were also analyzed in order to probe for changes in the transition from LA to the M_o photointermediate. The spectra of the LA (Figure 10, top) and the M_o state (Figure 10, middle) were obtained after subtracting the signal from the dark-adapted state of a natural-abundance bR sample acquired under identical experimental conditions. The carbon chemical shifts of the seven arginine residues in bR are within the ranges predicted from the model compounds. The LA − M_o difference spectrum (Figure 10, bottom) shows chemical shift changes in all resonances with the exception of C_ζ. (The dispersive line shapes at the ∼210 and ∼105 ppm positions of the C_ζ spinning sidebands reflect the small difference in the spinning speeds with which the two spectra were acquired.)

Figure 11 compares the ^{15}N CP/MAS spectra of the η resonances in the M_o state of bR with those of the neutral and alkaline forms of D85N. All of these forms of bR share the feature of the Arg 'wing' peaks. Specifically, we show the spectra of the M_o state of [$\eta_{1,2}$-$^{15}N_2$]Arg-bR in 0.1 M NaCl at pH 10.1, trapped at −44 °C (Figure 11, top), the dark-adapted M-like yellow form of [G-^{15}N]D85N in 0.3 M Gdn·HCl at pH 10.8 with 2 mM phosphate buffer (Figure

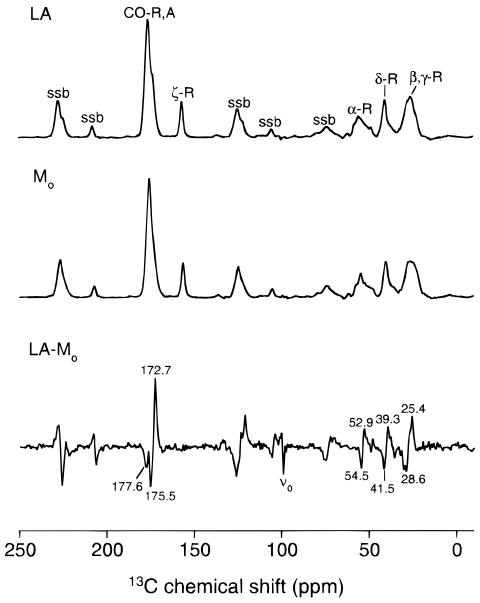

FIGURE 10: ^{13}C CP/MAS spectra of [1-^{13}C]Ala,[U-^{13}C,^{15}N]Arg,-[ζ-^{15}N]Lys-bR in 0.1 M NaCl, pH 10: LA state (top); M_o state (middle); and difference (bottom). ssb denotes a spinning sideband.

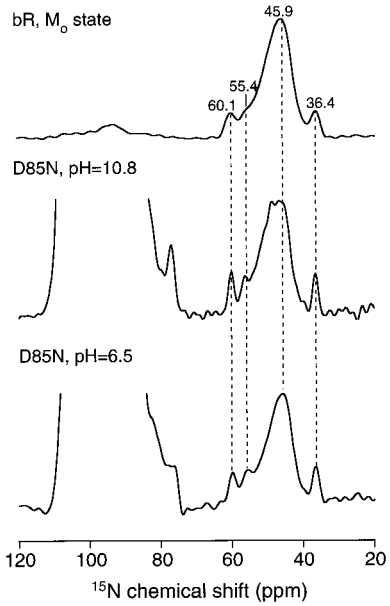

FIGURE 11: Comparison between the N_η resonances in WT bR and D85N: M_o state of [$\eta_{1,2}$-$^{15}N_2$]Arg-bR (WT) in 0.1 M NaCl at pH 10.1, accumulated at −44 °C (top); dark-adapted, M-like yellow form of [G-^{15}N]D85N in 0.3 M Gdn·HCl at pH 10.8 and 2 mM phosphate buffer (middle); and dark-adapted O-like blue form of [G-^{15}N]D85N in 0.1 M NaCl at pH 6.5 (bottom). The 'wing' peaks in all three spectra are virtually identical, with chemical shifts of 60.1/59.9 and 36.4 ppm. The striking resemblance between the arginine 'wing' peaks in the two CP/MAS spectra of D85N, regardless of the different protonation states of the SB, indicates that the protonation of Asp-85 might be the key to the presence of the 'wings'. The improved resolution in the D85N spectra is due to the use of a transmission line probe and TPPM decoupling during acquisition.

11, middle), and the dark-adapted O-like blue form of [G-^{15}N]D85N in 0.1 M NaCl at pH 6.5 (Figure 11, bottom). The 'wing' peaks in the three spectra are indistinguishable, with chemical shifts of 60.3 or 59.9 and 36.4 ppm. The smaller 'wing' peak intensity in the first spectrum is consistent with the percentage of the M_o state trapped under the aforementioned conditions. We have investigated the possibility that the nature of the halide in the salt medium might affect the 'wing' peaks in the WT M_o state of bR, and observed virtually no effect on either chemical shift when NaCl was replaced by NaBr and NaI (spectra not shown). The D85N mutant of bR provides the opportunity to completely exclude halide from the medium. For [G-^{15}N]-D85N bR suspended in 0.4 M HCOONa at pH 6 (λ_{max} = 603 nm compared to 606 nm in 0.1 M NaCl, pH 6.5), the same 'wing' peaks are observed (spectrum not shown) which further indicates that these η nitrogens do not interact with halide.

The delayed CP sequence (*59*) has been used to probe for protons in bacteriorhodopsin that exchange rapidly with bulk water, since the only protons with long T_2 relaxation times in hydrated purple membrane samples would be those of the bulk solvent. It has been reported (*59*) that the SB and the free N_ζ lysine signals persist after τ_d = 1 ms, τ_{CP} = 0.5−5 ms, while the amide resonances are suppressed. Another delayed CP study (τ_d = 1 ms, τ_{CP} = 1 ms) (*64*) showed that the arginine N_ϵ were absent at pH 7, but the downfield part of the resonance survived at pH 10. Using [1-^{13}C]Ala,[U-^{15}N]Arg,[ζ-^{15}N]Lys-bR in the current study permits the detection of the previously studied resonances together with the η nitrogens of the arginine residues. We have studied the effect of delayed CP on dark-adapted bR in 0.1 M NaCl at 23 °C [a 40:60 mixture of two species, bR_{568} (LA) and bR_{555}, respectively]. The ^{15}N spectra in Figure 12 compare standard CP and delayed CP at pH 7.4 and 10.1. The SB, the ζ lysine, the ϵ arginine, and the amide nitrogens were affected by the delayed CP as previously observed. In addition, the η arginine signal was suppressed at pH 7.4, while some of it survived at pH 10.1. These results reflect base-catalyzed exchange of the guanidyl protons with water (*65*, *66*). The relative peak intensities at pH 10.1 indicate that several of the arginine side chains are free to participate in base-catalyzed exchange. These do not include the residue responsible for the distinctive 55.6 ppm signal.

The delayed CP experiment was also carried out for [G-^{15}N]D85N in 0.1 M NaCl at pH ∼9.5. The standard CP spectrum at −80 °C is shown in Figure 13, top, and the delayed CP at 23 °C is shown below. Only part of the central arginine resonance survived the 1.1 ms delay. The signal-to-noise (S/N) in the bottom spectrum is not very high owing to fewer scans, and the requirement for a room temperature experiment to ensure sufficiently high proton T_2 and exchange rates. A smaller sample (because D85N pellets usually have higher water content compared to the WT) contributed to the lower S/N in the D85N spectra. The absence of 'wing' peak signals and the 55.4 ppm signal when CP is delayed indicates residues that are unable to participate in base-catalyzed exchange.

DISCUSSION

While ^{15}N solid-state NMR chemical shifts of arginine resonances could not be found in the literature, solution NMR data are available. Generally only a single resonance is observed for the η nitrogens in solution owing to fast N_η exchange by rotational diffusion about the N_ϵ−C_ζ bond. At pH <12 (below the guanidyl pK_a of ∼13), the chemical shifts of the N_η and N_ϵ are about 44−45 and 57−58 ppm,

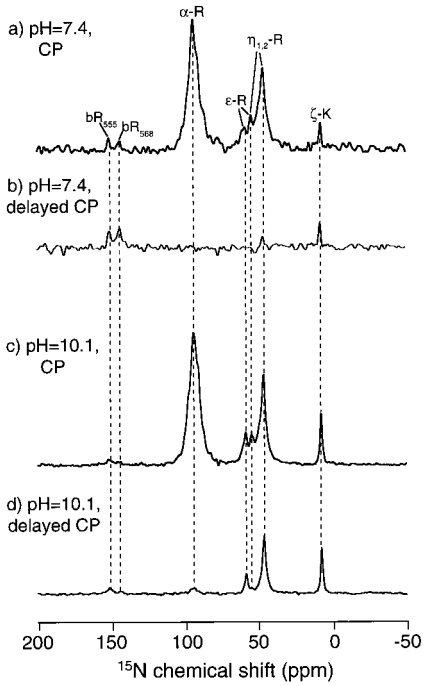

FIGURE 12: Delayed CP test of rapid proton exchange between bulk water and bR residues: ^{15}N CP/MAS spectra of the dark-adapted state of [1-^{13}C]Ala,[U-^{15}N]Arg, [ζ-^{15}N]Lys-bR in 0.1 M NaCl, $T = 23$ °C, 4.8 kHz spinning frequency: (a) standard CP at pH 7.4, $\tau_d = 0$ ms, $\tau_{CP} = 2$ ms, 5440 transients; (b) delayed CP at pH 7.4, $\tau_d = 0.82$ ms, $\tau_{CP} = 2$ ms, 36 800 transients; (c) standard CP at pH 10.1, $\tau_d = 0$ ms, $\tau_{CP} = 2$ ms, 16 640 transients; and (d) delayed CP at pH 10.1, $\tau_d = 0.82$ ms, $\tau_{CP} = 2$ ms, 27 520 transients. Resonances that survive delay in CP arise from nuclei that are cross-polarized by protons rapidly exchanged from bulk water. At pH 7.4, these are the SB and some of the free lysines N_ζ, while at pH 10.1 some of the arginine N_ϵ and N_η appear as well, but not the downfield N_η. The superior signal-to-noise ratio in both spectra at pH 10.1 seems to arise from increased CP efficiency to the arginine N_α and N_η and the lysine N_ζ resonances, and from base-catalyzed proton exchange when CP is delayed. Spectra a and c were acquired without the refocusing π pulse.

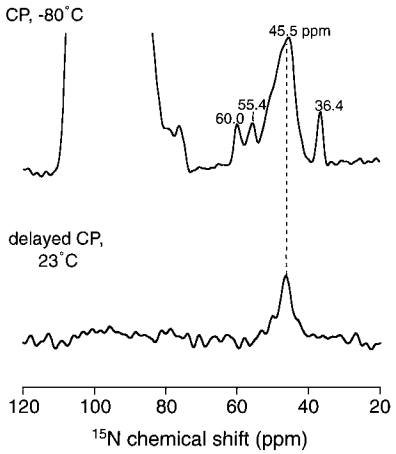

FIGURE 13: Proton exchange in a mixture of dark-adapted yellow, blue, and purple forms of [G-^{15}N]D85N in 0.1 M NaCl at pH ~9.5, $T = 23$ °C, 3.6 kHz spinning frequency: standard CP at −80 °C, $\tau_d = 0$ ms, $\tau_{CP} = 2$ ms, 40 960 transients (top); and delayed CP at 23 °C, $\tau_d = 1.1$ ms, $\tau_{CP} = 2$ ms, 17 280 transients (bottom). The lack of 'wing' peaks in the $\tau_d = 1.1$ ms case is consistent with a strongly interacting guanidyl group and/or a residue buried in the protein.

respectively, while at pH >14, deprotonation of the guanidyl group causes a downfield shift of both N_η and N_ϵ to about 60 and 62 ppm, respectively (*67*). However, at lower temperatures (with methanol or dimethyl sulfoxide added to prevent freezing), the rate of N_η exchange has been slowed sufficiently to allow observation of two distinct N_η resonances (*68*−*70*). For the protonated guanidyl group, the observed chemical shift separation was small (2.1−2.4 ppm). However, a very large separation (42.3 ppm) between the N_η's was observed for the deprotonated guanidyl group of arginine in DMSO/H_2O, pH 14.1 (*68*), presumably due to a very high degree of localization of the double bond. Observations of two η resonances (separated by 1.5−5.5 ppm) for arginine residues have been reported in several solution NMR structures of proteins (*69*, *71*−*73*), and are attributed to the formation of H-bonds, which increase both the asymmetry of the guanidyl group and the barrier for N_η exchange.

Among the solid compounds studied here, N-Ac-Arg·$2H_2O$ seems to be a good model system for the asymmetric environment of the guanidyl group in the M_o state of bR and D85N as indicated by the ^{15}N CP/MAS spectrum of *N*-[1-^{13}C]acetyl-[U-^{13}C,^{15}N]Arg·$2H_2O$ (Figure 2). Unfortunately, the crystal structure of this compound is not yet available. Nevertheless, from the existing crystal structures, Table 1, and general chemical shift considerations, some correlations might be established. Perturbation of the symmetric distribution of double bond character between the C−N bonds in the guanidyl group would lead to deshielding of a nitrogen forming a shorter C−N bond (more double bond character), and shielding of a nitrogen with a longer C−N bond. The effect of asymmetric interactions can be seen clearly in Arg-Asp·H_2O where a 9.1 ppm chemical shift difference between the η nitrogens is consistent with geometrically more favorable interactions of one of the η nitrogens with carboxylate oxygens (*48*). Perturbation of the symmetry of the guanidyl group, illustrated in shorter C_ζ−N_η bond lengths and closer $N_\eta\cdots Cl^-$ and $N_\eta\cdots O$ (carboxylate) contacts for one of the η nitrogens in the two crystallographically independent molecules of Arg·HCl (*43*), gives rise to large η_1 vs η_2 chemical shift differences. In Arg·HBr·H_2O and Arg·HCl·H_2O, with isomorphous crystal structures (*44*, *45*), the stronger proton acceptor (Br^- vs Cl^-) produces a larger η_1 vs η_2 chemical shift separation.

In WT bR the guanidyl nitrogens show change with a 1-in-7 stoichiometry in the transition between the resting state and the early M intermediate. The most dramatic shift is observed in the η position, where two 'wing' peaks flanking the central resonance arise. A 4 ppm upfield shift is detected in the ϵ position as well. The ^{13}C spectra show no changes in the ζ position, which is not surprising since the C_ζ chemical shift range in the model compounds is very small, and near-degeneracy of the C_ζ chemical shifts is observed in soluble proteins (*69*).

By utilizing rotor-synchronized CPDANTE inversion of the downfield 'wing' peak, and subsequent spin diffusion through the common proton reservoir, we have determined that the relative intensity of the 'wing' peaks is reduced by about 60% in 1.1 s. Except for the spin pairs included in the inverted peaks, essentially no decay after 1.1 s mixing has been detected in the central Arg resonance in the LA and M_o states. This suggests relatively long ^{15}N T_1's for the η nitrogens. Therefore, the decay observed in the 'wing' peaks in bR must be due to spin diffusion as in the model

compound. Considering the relative locations of the seven arginine side chains in bR, it becomes clear that such close contact between two η nitrogens could only take place if they belong to the same guanidyl group. We conclude that the WT M_o 'wing' peaks at 60.1 and 36.4 ppm arise from a single very asymmetric arginine residue in bR. We also note that the average chemical shift of the arginine 'wing' peaks, and of the rest of the η nitrogens, is 45−47 ppm. This indicates that the guanidyl groups of all seven residues remain protonated through the N state of the photocycle. This makes it highly unlikely that an arginine is the putative proton release group X proposed by Lanyi (*22*).

In principle, it should also be possible to use spin diffusion in order to correlate the η 'wing' peaks to the ϵ peak of the same guanidyl group in the M states (the three nitrogens being nearly equidistant from each other). However, the interaction between three coupled spins and the fact that the resonances of two of them nearly overlap (the downfield 'wing' falls in the range of the ϵ resonances) would complicate the analysis of the system.

The chemical shifts of the ϵ, η_1, and η_2 nitrogens in all the studied forms of WT bR and D85N fall in the range of the ϵ, η_1, and η_2 chemical shifts of the arginine-containing crystals. While none of them shows an η_1 vs η_2 difference as large as the 24 ppm seen for the 'wing' peaks in bR, some of the largest chemical shift separations between the η_1 and η_2 nitrogens were observed in the halide-containing arginine crystals. However, since we have found that the 'wing' peaks in bR are unaffected by substitution of Cl^- by Br^- or I^- or $HCOO^-$ we conclude that halide is not responsible for the large asymmetry in bR.

A second distinctively asymmetric arginine residue is associated with the 55.6 ppm shoulder in Figure 4. Since this signal is also inverted in the spin diffusion experiment, the signal of the other N_η in the same residue could be isolated at 45.4 ppm (Figure 8, top and middle spectra). The 10.2 ppm difference in this pair of peaks suggests the participation of one of the η nitrogens in a relatively strong interaction. Interestingly, both resonances of this Arg residue remain unaffected in all states that have been examined here. The only variation is that the line at 55.6 ppm, detected as a downfield shoulder in the LA and M_o spectra (Figure 4), is transformed into a tiny 'wing' peak, at 55.4 ppm, in the D85N spectra (Figures 11 and 13) due to improved resolution obtained by using a transmission line probe (*74*) and TPPM decoupling (*58*).

Delayed CP experiments (Figures 12 and 13) show that neither of the asymmetric arginine residues observed in the various forms of bR are able to participate in base-catalyzed proton exchange. This could be due to sequestration from solvent. But energetic considerations require that a buried, charged arginine be accompanied by an anion, and strong interaction with an anion, as is indicated by the large asymmetries of the N_η signals, would interfere with base-catalyzed exchange whether the arginine is buried or not.

The NMR spectroscopy of WT bR finds evidence for strong interactions of just one arginine residue in the resting state. Although the structural models of bR (*11*−*14*) suffer lower resolution near the protein surface, it is evident that no negatively charged residues are in the proximity of Arg-175 and Arg-225. The electron cryomicroscopy and X-ray diffraction models all show Arg-134 near Glu-194, but based on these models we cannot exclude the possibility of participation of Arg-7, Arg-164, and Arg-227 in salt bridges with Glu-9, Glu-166, and Asp-38 or Glu-166, respectively. Nevertheless, we tentatively assign the 55.6 ppm/45.4 ppm pair of NMR signals to Arg-134. The large difference in this pair of N_η chemical shifts is consistent with the asymmetry of the Arg-134/Glu-194 salt bridge in the model of Grigorieff et al. (*11*). There $N_{\eta 1}$ participates in a very strong H-bond with $O_{\epsilon 1}$, while $N_{\eta 2}$ is involved in much weaker interactions with $O_{\epsilon 1}$ and $O_{\epsilon 2}$ (due to unfavorable H-bond angles). It is noteworthy that CP/MAS spectra of the acid blue (pH 2 by HCl or pH 1.5 by H_2SO_4) and acid purple (pH 1.5 by H_2SO_4 with subsequent addition of NaCl) forms of WT bR lack the resonance at 55.6 ppm (spectra not shown). This observation is consistent with disruption of a salt bridge between Arg-134 and a surface carboxyl group, by protonation of the carboxyl at low pH.

In contrast to the 55.6/45.4 ppm pair of signals, the 60.1/36.4 ppm 'wing' peaks appear in the NMR spectra only when the charge of D85 is neutralized by proton transfer from the retinal SB in the M intermediate of the WT photocycle or by replacement of D85 with a neutral asparagine in the D85N mutant. The 'wing' peaks in D85N occur at both alkaline and neutral pH. Thus, they are unaffected by the protonation state of the SB or by the concomitant protein conformational changes observed in the electron density maps (*75*, *76*). This suggests that the 'wing' peaks are a local effect of neutralizing residue 85 and therefore might arise from Arg-82, just one helix turn away.

The location of the Arg-82 side chain has eluded the electron cryomicroscopy studies of bR (*10*−*12*), which would suggest weak interactions with other charged groups that might allow conformational disorder facilitated by the flexible arginine side chain (*10*, *11*). The X-ray structure shows a very weak H-bond between η_2 of Arg-82 and the side chain hydroxyl group of Thr-205. This scenario suggests that the ^{15}N η chemical shifts of Arg-82 in the resting state should deviate insignificantly from the average for a protonated guanidyl group, and, indeed, difference spectra (bottom of Figure 4) show that the chemical shifts in the LA state of the nuclei from which the M state 'wing' peaks originate are 48.1 and 45.9 ppm. The unusual asymmetry of the guanidyl group in the M-state and D85N (manifested in the 24 ppm chemical shift separation between $N_{\eta 1}$ and $N_{\eta 2}$) is suggestive of a strong H-bonding or ion pair interaction of at least one nitrogen, most likely with a carboxyl group. (Having excluded an interaction with the halide, the only possibilities remaining are a carboxyl group or a water molecule, and the last alone would be insufficient to provide such a strong asymmetry.) Significantly, distinct 'wing' peaks are not found in the spectra of acid blue and acid purple forms of bR, where Asp-85 is protonated as in M and D85N (results not shown). This suggests that the 'wing' peaks depend on interaction with a carboxyl group that becomes protonated at low pH.

The assignment of the 'wing' peaks to Arg-82 is consistent with participation of Arg-82 in the Schiff base counterion complex in LA (together with Asp-85, Asp-212, and some water) and with the disappearance of the IR continuum in the M photocycle intermediate (*77*), which has been associated with restructuring of interactions in the extracellular half of the proton channel. Since the change that we assign to

Arg-82 occurs already in the early (M_o) state, it probably does not act as the reprotonation "switch" of the WT bR photocycle. However, it might stabilize proton transfer from the SB to Asp-85 and relay the effect to the extracellular proton release group. This interpretation is also consistent with the effects of Arg-82 mutations on the photocycle kinetics and with the evidence that Arg-82 controls the pK_a's of Asp-85 and the proton release group at the extracellular side (*27*−*31*, *78*).

Molecular dynamics simulations (*35*, *36*, *79*, *80*) paint two very different scenarios for Arg-82 in the photocycle. In both cases, Arg-82 begins the cycle interacting with Asp-212 and Asp-85. However, the behavior is completely distinct after proton transfer from the SB to Asp-85. In one case (*35*, *36*), the Arg-82 side chain swings toward E204 on the extracellular side of the membrane with H-bonding to T205. In the other case (*79*, *80*), Arg-82 remains close to Asp-85 and Asp-212. What the present NMR data suggest is that, whether the Arg-82 side chain moves or not, the interactions of Arg-82 are nearly symmetric at the start of the photocycle and extraordinarily asymmetric after SB deprotonation.

CONCLUSIONS

Perturbation of one of the seven arginine side chains in the LA→M_o transition of bR is evident for all guanidyl group nitrogen atoms. It is most pronounced for the η-^{15}N where two 'wing' peaks emerge at 60.1 and 36.4 ppm. At the same time, a 4 ppm upfield shift is observed in one ϵ-^{15}N resonance. The 24 ppm chemical shift difference between the η resonances of the perturbed arginine side chain indicates a change to an unusually asymmetric environment. In model compounds, the asymmetries are all smaller, except in the case of complete deprotonation of the guanidyl group at high pH where it is larger.

The same η-^{15}N 'wing' peaks, corresponding to a single arginine residue, are observed in the early and late M states of WT bR, where Asp-85 has been protonated from the SB, and in the D85N mutant of bR, where the charge at residue 85 has been neutralized by mutation. The presence of the 'wing' peaks in D85N independent of the protonation state of the Schiff base (i.e., at both neutral and high pH) suggests that the absence of a negative charge at residue 85 is the key to the guanidyl group asymmetry and provides a strong indication that Arg-82 is responsible for the rise of the 'wing' peaks in the early and late M states of bR.

The absence of the 'wing' peaks in acid blue WT bR, despite the protonation of Asp-85 in this state, suggests that the 'wing' peaks depend on interaction with another carboxyl group that also becomes protonated at low pH. This is consistent with a scenario for Arg-82 that has been developed in molecular dynamics simulations.

The only other significantly asymmetric arginine residue shows a 10 ppm difference between its η resonances, equally in all WT and D85N states except those at low pH. This is tentatively assigned to Arg-134 based on structural evidence for asymmetric interactions between this residue and a surface carboxyl group which would be released when the carboxyl group is protonated at low pH.

ACKNOWLEDGMENT

We thank Drs. Boqin Sun and Hong Ni for helpful discussions, Prof. R. Needleman for providing the D85N bR strain of *H. salinarium*, Prof. J. Rosenbusch and colleagues for providing their X-ray structure coordinates, and Prof. C. Scharnagl and Prof. C. Schulten for sharing the coordinates of simulated photointermediates. K. V. Lakshmi's Ph.D. Thesis (*64*) has been a valuable reference about arginine and bR. Thanks are accorded also to Chad Rienstra for the design of the transmission line probe employed in these experiments.

REFERENCES

1. Capitani, J. F., and Pedersen, L. (1978) *Chem. Phys. Lett. 54*, 547−550.
2. Mrabet, N. T., Van den Broeck, A., Van den Brande, I., Stanssens, P., Laroche, Y., Lambeir, A.-M., Matthijssens, G., Jenkins, J., Chiadmi, M., van Tilbeurgh, H., Rey, F., Janin, J., Quax, W. J., Lasters, I., Maeyer, M. D., and Wodak, S. J. (1992) *Biochemistry 31*, 2239−2253.
3. Salunke, D. M., and Vijayan, M. (1981) *Int. J. Pept. Protein Res. 18*, 348−351.
4. Patthy, L., and Smith, E. L. (1975) *J. Biol. Chem. 250*, 565−569.
5. Riordan, J. F., McElvany, K. D., and Borders, C. L. (1977) *Science 195*, 884−886.
6. Cotton, F. A., la Cour, T., Hazen, E. E., and Legg, M. J. (1977) *Biochim. Biophys. Acta 481*, 1−5.
7. Knowles, J. R. (1980) *Annu. Rev. Biochem. 49*, 877−919.
8. Pavletich, N. P., and Pabo, C. O. (1991) *Science 252*, 809−817.
9. Omichinski, J. G., Clore, G. M., Schaad, O., Felsenfeld, G., Trainor, C., Appella, E., Stahl, S. J., and Gronenborn, A. M. (1993) *Science 261*, 438−446.
10. Henderson, R., Baldwin, J. M., Ceska, T. A., Zemlin, F., Beckmann, E., and Downing, K. H. (1990) *J. Mol. Biol. 213*, 899−929.
11. Grigorieff, N., Ceska, T. A., Downing, K. H., Baldwin, J. M., and Henderson, R. (1996) *J. Mol. Biol. 259*, 393−421.
12. Kimura, Y., Vassylyev, D. G., Miyazawa, A., Kidera, A., Matsushima, M., Mitsuoka, K., Murata, K., Hirai, T., and Fujiyoshi, Y. (1997) *Nature 389*, 206−211.
13. Pebay-Peyroula, E., Rummel, G., Rosenbusch, J. P., and Landau, E. M. (1997) *Science 277*, 1676−1681.
14. Luecke, H., Richter, H.-T., and Lanyi, J. K. (1998) *Science 280*, 1934−1937.
15. Braiman, M. S., Mogi, T., Stern, L. J., Hackett, N. R., Chao, B. H., Khorana, H. G., and Rothschild, K. J. (1988) *Proteins: Struct., Funct., Genet. 3*, 219−229.
16. Braiman, M. S., Mogi, T., Marti, T., Stern, L. J., Khorana, H. G., and Rothschild, K. J. (1988) *Biochemistry 27*, 8516−8520.
17. Gerwert, K., Hess, B., Soppa, J., and Oesterhelt, D. (1989) *Proc. Natl. Acad. Sci. U.S.A. 86*, 4943−4947.
18. de Groot, H. J. M., Harbison, G. S., Herzfeld, J., and Griffin, R. G. (1989) *Biochemistry 28*, 3346−3353.
19. Hatanaka, M., Sasaki, J., Kandori, H., Ebrey, T. G., Needleman, R., Lanyi, J. K., and Maeda, A. (1996) *Biochemistry 35*, 6308−6312.
20. Khorana, H. G., Gerber, G. E., Herlihy, W. C., Gray, C. P., Anderegg, R. J., Nibei, K., and Biemann, K. (1979) *Proc. Natl. Acad. Sci. U.S.A. 76*, 5046−5050.
21. Rothschild, K. J. (1992) *J. Bioenerg. Biomembr. 24*, 147−167.
22. Lanyi, J. K. (1993) *Biochim. Biophys. Acta 1183*, 241−261.
23. Stern, L. J., and Khorana, H. G. (1989) *J. Biol. Chem. 264*, 14202−14208.
24. Lin, G. C., El-Sayed, M. A., Marti, T., Stern, L. J., Mogi, T., and Khorana, H. G. (1991) *Biophys. J. 60*, 172−178.
25. Feng, Y., Chen, N., Hazard, E. S., Misra, S., Ebrey, T. G., Menick, D. R., and Crouch, R. K. (1995) *Biophys. J. 68*, A334.
26. Misra, S., Martin, C., Kwon, O.-H., Ebrey, T. G., Chen, N., Crouch, R. K., and Menick, D. R. (1997) *Photochem. Photobiol. 66*, 774−783.
27. Balashov, S. P., Govindjee, R., Kono, M., Imasheva, E., Lukashev, E., Ebrey, T. G., Crouch, R. K., Menick, D. R., and Feng, Y. (1993) *Biochemistry 32*, 10331−10343.

28. Balashov, S. P., Govindjee, R., Imasheva, E. S., Misra, S., Ebrey, T. G., Feng, Y., Crouch, R. K., and Menick, D. R. (1995) *Biochemistry 34*, 8820−8834.
29. Govindjee, R., Misra, S., Balashov, S. P., Ebrey, T. G., Crouch, R. K., and Menick, D. R. (1996) *Biophys. J. 71*, 1011−1023.
30. Balashov, S. P., Imasheva, E. S., Ebrey, T. G., Crouch, R. K., Chen, N., and Menick, D. R. (1998) *Biophys. J. 74*, A293.
31. Balashov, S. P., Imasheva, E. S., Govindjee, R., and Ebrey, T. G. (1996) *Biophys. J. 70*, 473−481.
32. Richter, H.-T., Brown, L. S., Needleman, R., and Lanyi, J. K. (1996) *Biochemistry 35*, 4054−4062.
33. Balashov, S. P., Imasheva, E. S., Ebrey, T. G., Chen, N., Menick, D. R., and Crouch, R. K. (1997) *Biochemistry 36*, 8671−8676.
34. Scharnagl, C., Hettenkofer, J., and Fischer, S. F. (1994) *Int. J. Quantum Chem. Quantum Biol. Symp. 21*, 33−56.
35. Scharnagl, C., Hettenkofer, J., and Fischer, S. F. (1995) *J. Phys. Chem. 99*, 7787−7800.
36. Scharnagl, C., and Fischer, S. F. (1996) *Chem. Phys. 212*, 231−246.
37. Genick, U. K., Borgstahl, G. E. O., Ng, K., Ren, Z., Pradervand, C., Burke, P. M., Srajer, V., Teng, T.-Y., Schildkamp, W., McRee, D. E., Moffat, K., and Getzoff, E. D. (1997) *Science 275*, 1471−1475.
38. Turner, G. J., Miercke, J. W., Thorgeirsson, T. E., Kliger, D. S., Betlach, M. C., and Stroud, R. M. (1993) *Biochemistry 32*, 1332−1337.
39. Dickopf, S., Alexiev, U., Krebs, M. P., Otto, H., Mollaaghababa, R., Khorana, H. G., and Heyn, M. P. (1995) *Proc. Natl. Acad. Sci. U.S.A. 92*, 11519−11523.
40. Moltke, S., Krebs, M. P., Mollaaghababa, R., Khorana, H. G., and Heyn, M. P. (1995) *Biophys. J. 69*, 2074−2083.
41. Nilsson, A., Rath, P., Olejnik, J., Coleman, M., and Rothschild, K. J. (1995) *J. Biol. Chem. 270*, 29746−29751.
42. Lehmann, M. S., Verbist, J. J., Hamilton, W. C., and Koetzle, T. F. (1973) *J. Chem. Soc., Perkin Trans. 2 1973*, 133−137.
43. Mazumdar, S. K., Venkatesan, K., Mez, H.-C., and Donohue, J. (1969) *Z. Kristallogr. 130*, 328−339.
44. Dow, J., Jensen, L. H., Mazumdar, S. K., Srinivasan, R., and Ramachandran, G. N. (1970) *Acta Crystallogr. B26*, 1662−1671.
45. Mazumdar, S. K., and Srinivasan, R. (1966) *Z. Kristallogr. 123*, 186−205.
46. Aoki, K., Nagano, K., and Iitaka, Y. (1971) *Acta Crystallogr. B27*, 11−23.
47. Yokomori, Y., and Hodgson, D. (1988) *Acta Crystallogr. C44*, 521−525.
48. Eggleston, D. S., and Hodgson, D. J. (1985) *Int. J. Pept. Protein Res. 25*, 242−253.
49. Sudhakar, V., and Vijayan, M. (1980) *Acta Crystallogr. B36*, 120−125.
50. Greenstein, J. P., and Winitz, M. (1961) *Chemistry of the Amino Acids*, Wiley, New York.
51. Gochnauer, M. B., and Kushner, D. J. (1969) *Can. J. Microbiol. 15*, 1157−1165.
52. Miller, G. H. (1972) *Experiments in Molecular Genetics*, Cold Spring Harbor Laboratory, Cold Spring Harbor, NY.
53. Gerhardt, P. (1981) *Manual of Methods for General Bacteriology*, American Society for Microbiology, Washington, D.C.
54. Oesterhelt, D., and Stoeckenius, W. (1974) *Methods Enzymol. 31*, 667−678.
55. Hu, J. G., Sun, B. Q., Petkova, A. T., Griffin, R. G., and Herzfeld, J. (1997) *Biochemistry 36*, 9316−9322.
56. Bielicki, A., and Burum, D. P. (1995) *J. Magn. Reson. A 116*, 215−220.
57. Pines, A., Gibby, M. G., and Waugh, J. S. (1973) *J. Chem. Phys. 59*, 569−590.
58. Bennett, A. E., Rienstra, C. M., Auger, M., Lakshmi, K. V., and Griffin, R. G. (1995) *J. Chem. Phys. 103*, 1−8.
59. Harbison, G. S., Roberts, J. E., Herzfeld, J., and Griffin, R. G. (1988) *J. Am. Chem. Soc. 110*, 7221−7223.
60. Kubo, A., and McDowell, C. A. (1988) *J. Chem. Soc., Faraday Trans. 1 84*, 3713−3730.
61. Harbison, G. S., Herzfeld, J., and Griffin, R. G. (1983) *Biochemistry 22*, 1−5.
62. Lakshmi, K. V., Farrar, M. R., Raap, J., Lugtenburg, J., Griffin, R. G., and Herzfeld, J. (1994) *Biochemistry 33*, 8853−8857.
63. Hu, J. G., Sun, B. Q., Bizounok, M., Hatcher, M. E., Lansing, J. C., Raap, J., Verdegem, P. J. E., Lugtenburg, J., Griffin, R. G., and Herzfeld, J. (1998) *Biochemistry 37*, 8088−8096.
64. Lakshmi, K. V. (1994) Ph.D. Thesis, Brandeis University,
65. Wüthrich, K. (1986) *NMR of Proteins, and Nucleic Acids*, John Wiley, and Sons, New York.
66. Liepinsh, E., and Otting, G. (1996) *Magn. Reson. Med. 35*, 30−42.
67. Levy, G. C., and Lichter, R. L. (1979) *Nitrogen-15 Nuclear Magnetic Resonance Spectroscopy*, Wiley-Interscience, New York.
68. Kanamori, K., and Roberts, J. D. (1983) *J. Am. Chem. Soc. 105*, 4698−4701.
69. Yamazaki, T., Pascal, S. M., Singer, A. U., Forman-Kay, J. D., and Kay, L. E. (1995) *J. Am. Chem. Soc. 117*, 3556−3564.
70. Henry, G. D., and Sykes, B. D. (1995) *J. Biomol. NMR 5*, 59−66.
71. Pascal, S. M., Yamazaki, T., Singer, A. U., Kay, L. E., and Forman-Kay, J. D. (1995) *Biochemistry 34*, 11353−11362.
72. Nieto, P. M., Birdsall, B., Morgan, W. D., Frenkiel, T. A., Gargaro, A. R., and Feeney, J. (1997) *FEBS Lett. 405*, 16−20.
73. Starich, M. R., Omichinski, J. G., Pedone, P. V., Felsenfeld, G., Gronenborn, A. M., and Clore, G. M. (1998) *The solution structure of the N-terminal GATA-2 DNA binding domain complexed with a consensus GATA target*, Asilomar, CA.
74. Rienstra, C. M., Gamburg, A., Gross, G. D., Hu, J. G., Itin, B., Rovnyak, D. S., and Griffin, R. G. (1998) (to be submitted for publication).
75. Kataoka, M., Kamikubo, H., Tokunaga, F., Brown, L. S., Yamazaki, Y., Maeda, A., Sheves, M., Needleman, R., and Lanyi, J. K. (1994) *J. Mol. Biol. 243*, 621−638.
76. Brown, L. S., Kamikubo, H., Zimanyi, L., Kataoka, M., Tokunaga, F., Verdegem, P., Lugtenburg, J., and Lanyi, J. K. (1997) *Proc. Natl. Acad. Sci. U.S.A. 94*, 5040−5044.
77. Rammelsberg, R., Huhn, G., Lübben, M., and Gerwert, K. (1998) *Biochemistry 37*, 5001−5009.
78. Subramaniam, S., Marti, T., and Khorana, H. G. (1990) *Proc. Natl. Acad. Sci. U.S.A. 87*, 1013−1017.
79. Zhou, F., Windemuth, A., and Schulten, K. (1993) *Biochemistry 32*, 2291−2306.
80. Xu, D., Sheves, M., and Schulten, K. (1995) *Biophys. J. 69*, 2745−2760.
81. Long, J. R., Sun, B. Q., Bowen, A., and Griffin, R. G. (1994) *J. Am. Chem. Soc. 116*, 11950−11956.

BI981968Z